

# Magnetization Dynamics in a Perpendicular Anisotropy Free Layer under a Spin Torque Effect with Crossed Polarization

Nafeesa Rahman and Rachid Sbiaa\*

Department of Physics, College of Science, Sultan Qaboos University, P.O. Box 36, Al-Khoud, PC 123, Muscat, Sultanate of Oman. \*Email: rachid@squ.edu.om.

**ABSTRACT:** The transfer of spin angular momentum from a spin polarized current provides an efficient way of reversing the magnetization direction of the free layer of the magnetic tunnel junction (MTJ), and while faster reversal will reduce the switching energy, this in turn will lead to low power consumption. In this work, we propose a design where a spin torque oscillator (STO) is integrated with a conventional magnetic tunnel junction (MTJ) which will assist in the ultrafast reversal of the magnetization of the free layer of the MTJ. The structure formed (MTJ stacked with STO), will have the free layer of the MTJ sandwiched between two spin polarizer layers, one with a fixed magnetization direction perpendicular to film plane (main static polarizer) and the other with an oscillatory magnetization (dynamic polarizer). The static polarizer is the fixed layer of the MTJ itself and the dynamic polarizer is the free layer of the STO.

**Keywords:** Magnetic random access memory; Spin transfer torque; Magnetization reversal; Magnetic tunnel junction; Spin torque oscillator.

دراسة حركة المغنطة المغناطيسية في العينات ذات المغنطة العمودية بتأثير عزم إلكترونيات التيار الكهربائي

نفيسة عناية الرحمان و رشيد سبيع

**المخلص:** سيساعد مذبذب عزم الدوران (STO) عند دمجها مع تقاطع النفق المغناطيسي التقليدي (MTJ) في الانعكاس فائق السرعة لمغناطيسية الطبقة الحرة من MTJ. سيكون للهيكل المكون (MTJ مكعدة بـ STO) طبقة حرة من MTJ محصورة بين طبقتين مستقطبتين. احداها ذات اتجاه مغناطيسي ثابت عمودي على مستوى فيلم (مستقطب ثابت رئيسي) والآخر مع مغنطة تذبذبية (مستقطب ديناميكي). المستقطب الثابت هو الطبقة الثابتة من MTJ نفسها والمستقطب الديناميكي هو الطبقة الحرة من STO.

**الكلمات المفتاحية:** ذاكرة الوصول العشوائي المغناطيسية، نقل تدور عزم الدوران، تبديل المغناطيس، الجهاز النفقي المغناطيسي، دوران الإلكترون.



## 1. Introduction

Spin transfer torque (STT) in magnetic heterostructures gives rise to several dynamical processes that are not accessible with a magnetic field alone [1-5]. Two such magnetic heterostructures are the Magnetic Tunnel Junction (MTJ) and a Spin Torque Oscillator (STO). Both MTJ and STO comprise a magnetic free layer (FL), a magnetic reference layer (RL) and a non-magnetic layer between them. The use of MTJ in Random Access Memory (RAM) application leads to magnetic RAM (MRAM). When the damping is overcome by the spin angular momentum the magnetization of the free layer could be reversed between its two equilibrium states. This is the principle of writing in

STT-MRAM. Magnetic tunnel junction with perpendicular magnetic anisotropy has experienced strong growth in the past 10 years and has a good potential for the future growth of low power consumption and high-density STT-MRAM [6-16]. In STT-MRAM, the magnetic state of an MTJ is switched by applying a spin-polarized current through the junction. The magnetization switching of the free layer of the MTJ occurs only when the current density exceeds the threshold current, also known as the critical current or, more specifically, critical current density,  $J_c = i_c/A$  (where  $i_c$  is the critical current and  $A$  is the area of the MTJ). At a given current ( $i \geq i_c$ ), the minimum pulse width needed to switch the magnetization is defined as the switching time  $t_s$ . The goal of low power magnetic memory involves reducing the critical current as well as switching time of the MTJ.

An STO exhibits self-sustained magnetization oscillations, which are made possible through the compensation of magnetic damping by the transfer of spin angular momentum from a spin-polarized current [17-23]. When magnetization dynamics are induced in the active layer, the magnetoresistance of the device becomes time-varying, thereby generating a microwave signal. Thus, an STO has the capability of converting a direct current into a microwave signal, by utilizing the spin transfer torque (STT) in ferromagnetic multilayer systems. More recently, and to store more data in a magnetic nanowire, it has been discovered that spin torque could also move domain wall, leading thus to different magnetic states [24-36]. An STO which is a spintronic device is fabricated without any semiconductor material [37]. It is a nanoscopic and ultra-tunable microwave signal generator. The microwave signals emitted by an STO can vary in frequency from hundreds of MHz to 40 GHz. The frequency of emission is a function of the magnitude and direction of the dc spin-polarized current. If in addition to the spin-polarized current, an external magnetic field is applied, then the frequency generally increases with the applied magnetic field because the magnetic oscillations are precessional: The larger the net effective magnetic field, the greater the torque acting on the spins, and the higher the frequency of precession. The frequency of emission is also a function of the strength and angle of the applied magnetic field.

In this paper a technique is presented, wherein a spin torque oscillator with an optimal frequency is integrated with a conventional MTJ to realize a real-time device known as a ‘‘Spin Transfer Oscillator Magnetic Tunnel Junction’’ (STOMTJ), which will form the basis for low power magnetic memory [38-40]. In our proposed methodology, a STOMTJ nanostructure is formed by stacking an STO and an MTJ vertically, separated by a spacer. The magnetization of FL of MTJ, if aligned parallel or antiparallel with respect to its own fixed layer magnetization corresponds to binary bit 1 and binary bit 0 as shown in Figure 1(a).

The STO used in the STOMTJ device is a trilayer structure comprising a magnetic FL, a magnetic RL and a non-magnetic layer between them. The magnetization direction of the FL initially in-plane can be changed under a polarized electric current while the direction of the RL magnetization is unchangeable and aligned in the  $z$ -direction. The simulation results of such an STO are enumerated elsewhere [41]. The spin-polarized d.c current injection is capable of inducing oscillations in the free layer of the STO. The free layer of the STO acts as a resonance-inducing-polarizer, effectively reducing the critical current of the MTJ in the STOMTJ device. This reduction of the critical current can improve the performance of the MTJ leading to low power magnetic memory. The magnetization reversal of the free layer of MTJ results from the contribution of two polarizers as shown in Figure 1(b), where the magnetizations  $\mathbf{m}_{p1}$  and  $\mathbf{m}_{p2}$  are considered to be a static polarizer and dynamic polarizer, respectively. The RL and the non-magnetic layer of the STO are not shown in Fig 1(b) for simplicity.

## 2. Theoretical model

In the first case, an MTJ is simulated as shown in Fig. 1 (a). The magnetization direction of the FL ( $\mathbf{m}$ ) can be changed under a polarized electric current while the direction of the RL magnetization ( $\mathbf{m}_p$ ) is unchangeable and aligned in the  $z$ -direction. The dynamics of the magnetization of the free layer in the presence of spin-polarized current is obtained by solving the LLGS equation given by Eq. 1.

$$\frac{d\mathbf{m}}{dt} = \gamma[\mathbf{m} \times \mathbf{H}_{\text{eff}}] + \alpha \left( \mathbf{m} \times \frac{d\mathbf{m}}{dt} \right) \quad (1)$$

In Eq. 1,  $\gamma$  is the gyromagnetic ratio,  $\alpha$  is the damping constant,  $\mathbf{m}$  is the normalized magnetization of the free layer. The effective field  $\mathbf{H}_{\text{eff}}$  can be expressed by

$$\mathbf{H}_{\text{eff}} = \mathbf{H}_s + \mathbf{H}_k + \mathbf{H}_{\text{ex}} + \mathbf{H}_{\text{ST}} \quad (2)$$

In Eq. 2,  $\mathbf{H}_s$  is the magnetostatic field,  $\mathbf{H}_k$  is the magnetic anisotropy field,  $\mathbf{H}_{\text{ex}}$  is the exchange field and  $\mathbf{H}_{\text{ST}}$  is the spin transfer torque field given by Eq. 3.

$$\mathbf{H}_{\text{ST}} = -H_{\text{ST}}(\mathbf{m} \times \mathbf{m}_p) \quad (3)$$

In Eq. 3,  $\mathbf{m}_p$  is a vector with polarization direction of the reference layer,  $H_{\text{ST}}$  is given by Eq. 4 where  $J$  is the current density ( $J = i/A$ ),  $t$  is the thickness of the ferromagnetic layer under STT,  $\varepsilon$  is the spin polarization efficiency,  $M_s$  is the saturation magnetization,  $e$  is the electron charge and  $\hbar$  is the reduced Planck constant.

$$H_{ST} = \frac{\hbar \varepsilon J}{2eM_s t} = \frac{\hbar \varepsilon i}{2eM_s t A} \quad (4)$$

### 3. Results and discussion

#### Case 1: MTJ simulation without dynamic polarizer.

For solving Eq. 1, the free layer of the device MTJ, with a size of  $30 \times 30 \times 2 \text{ nm}^3$  and discretization of  $3 \times 3 \times 2 \text{ nm}^3$  was considered. The polarization vector  $\mathbf{m}_p$  is in the positive  $z$ -direction following the orientation of the magnetization of the perpendicular polarizer. The free layer saturation magnetization ( $M_s$ ), spin current polarization ( $P$ ), the anisotropy field ( $H_k$ ) and exchange stiffness constant ( $A$ ) were fixed to 600 kA/m, 0.6, 900 mT and  $4 \times 10^{-12} \text{ J/m}$ , respectively. By exploring magnetization dynamics at different values of current, the critical current ( $i_c$ ) was found to be 0.2 mA with switching time ( $t_s$ ) of 0.5 ns, as shown in Figure 2. As can be easily understood, a current with magnitude more than the critical current  $i_c$  led to a decrease in the MTJ switching time.

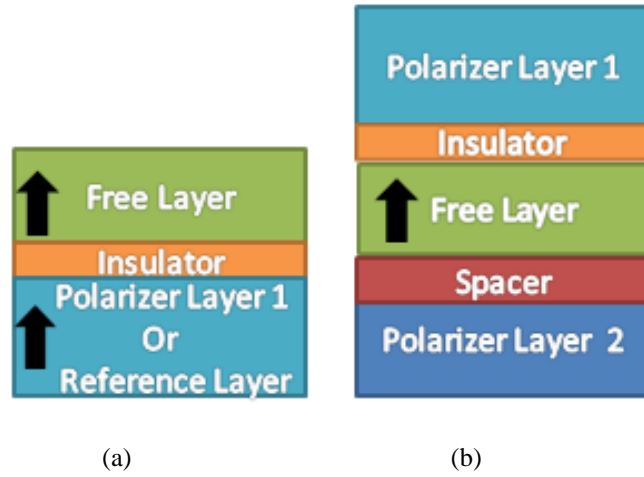


**Figure 1.** (a) The sketch of the p-MTJ and (b) the sketch of the p-MTJ with two spin polarizer layers.

#### Case 2: MTJ simulation with dynamic polarizer.

In the second part of this study, the magnetization dynamics of the free layer shown in Figure 1 (b) was investigated. In this scheme, the free layer magnetization  $\mathbf{m}$  was under two spin-transfer torque fields. The first one was  $\mathbf{H}_{ST1}$ , from the main static polarizer ( $\mathbf{m}_{p1}$ ), with a fixed magnetization direction, which was taken in the positive  $z$ -axis (out-of-plane). The second STT field  $\mathbf{H}_{ST2}$  was from the second polarizer layer ( $\mathbf{m}_{p2}$ ) which is the free layer of an STO here considered to be a dynamic polarizer. Its magnetization, given by Eq. 5, is oscillating at a characteristic frequency depending on the intrinsic properties of the STO and applied current. In Eq. 5,  $M_s$  is the saturation magnetization of the free layer of the dynamic polarizer,  $f$  is its oscillation frequency and  $\theta$  is the angle between the out of plane axis ( $z$ -axis) and its magnetization vector. The spin torque efficiency from the polarizer  $\mathbf{m}_{p2}$  was fixed to 0.3.

$$\mathbf{m}_{p2} = M_s (\sin\theta \cos(2\pi f t) \hat{\mathbf{e}}_x + \sin\theta \sin(2\pi f t) \hat{\mathbf{e}}_y + \cos\theta \hat{\mathbf{e}}_z) \quad (5)$$

The second STT field  $\mathbf{H}_{ST2}$  was obtained by substituting Eq. 5 in Eq. 3. The magnitude of the  $\mathbf{H}_{ST2}$  is given by equation 4. For the STO-MTJ device shown in Figure 1 (b), the magnetization dynamics were explored at different values of current. The critical current ( $i_c$ ) was found to be 0.1 mA with switching time ( $t_s$ ) of 0.5 ns, as shown in the Figure 3. The spin-polarized d.c current injection is capable of inducing oscillations in the free layer of the STO. The magnetization of the dynamic polarizer was oscillating at 7 GHz and  $\theta = 85^\circ$ . Without the dynamic polarizer, the magnetization of the free layer of MTJ was precessing and then going back to its initial magnetization state. It is important to note that for the current value  $i = 0.1 \text{ mA}$ , the switching of the free layer magnetization  $\mathbf{m}$  with only the main polarizer, similar to an MTJ device only, was not possible, as shown in Fig. 4(a). With the dynamic polarizer, the precessing  $\mathbf{m}$  was in synchronization with  $\mathbf{m}_{p2}$ , and the resonance condition was achieved leading to magnetization reversal as shown in Figure 4(b).

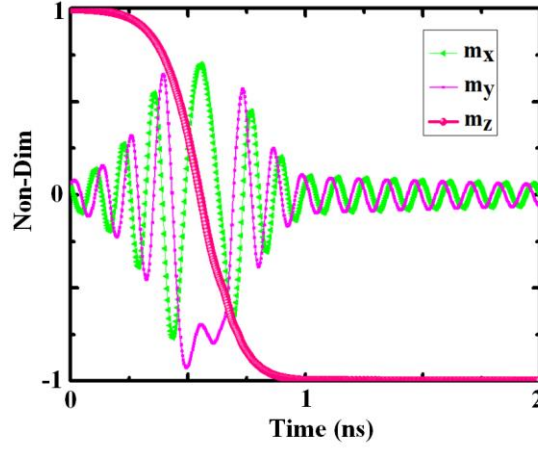


**Figure 2.** Time domain plot of the three normalized components of the magnetization ( $m_x$ ,  $m_y$  and  $m_z$ , respectively represented in green, purple and pink) with respect to time for  $I = 0.2$  mA.

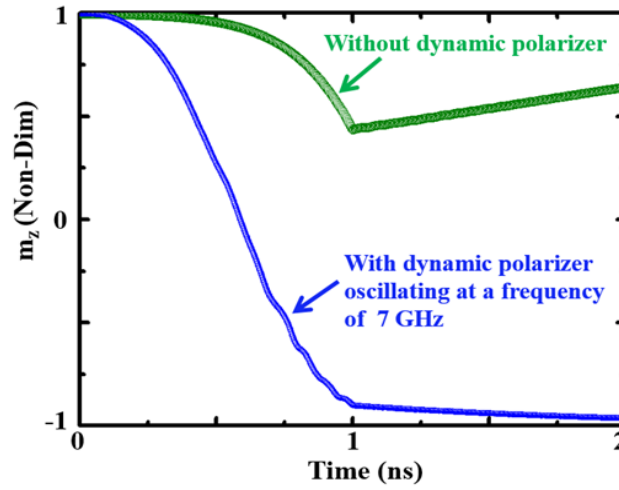


**Figure 3.** Time domain plot of the normalized component of the magnetization  $m_z$  for  $i = 0.1$  mA.

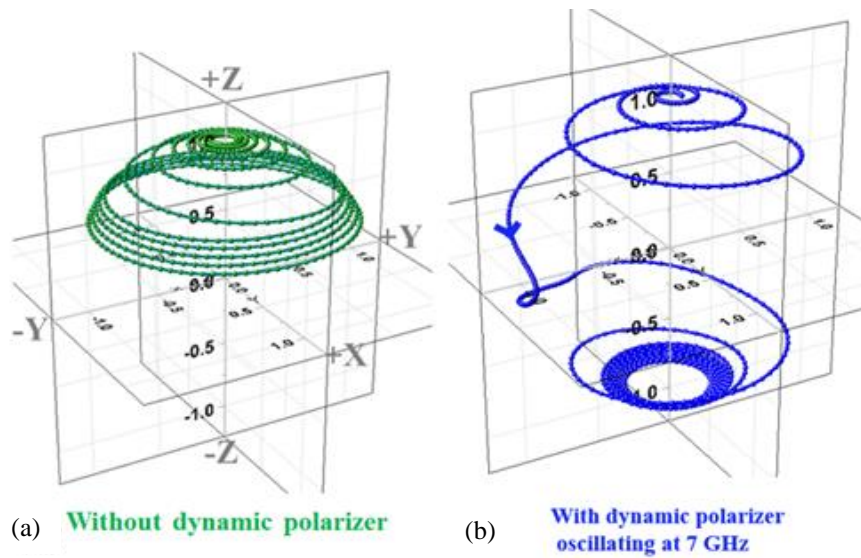


**Figure 4.** The trajectory of magnetization vector for  $i = 0.1$  mA (a) without dynamic polarizer and (b) with dynamic polarizer oscillating at  $f = 7$  GHz.

In comparison to magnetization switching by ferromagnetic resonance (FMR) and STT-FMR, the resonance in the STO-MTJ device is without the use of a.c. current  $i_{r,f}$ . The dynamic magnetization  $\mathbf{m}_{p2}$  has a microwave component

at the FMR frequency and the associated STT drives  $\mathbf{m}$  into resonance. Thus, the driving force of the magnetic precession in STT-FMR in a magnetic tunnel junction device is the oscillating  $\mathbf{m}_{p2}$  associated with an applied spin-polarized d.c current  $i_{d.c}$ . The frequency of the oscillating  $\mathbf{m}_{p2}$  can be tuned by adjusting the STO's fixed and oscillating layers' properties such as their spin polarization, thickness, anisotropy field and saturation magnetization. The area of the STO and magnitude of the current passing through it will be the same as the MTJ device.

An MTJ as shown in Figure 1 is made of ultra-thin films with a thickness of 2 nm or less. In general, the insulator layer and the magnetic layer are made of MgO and CoFeB alloy respectively. To validate the design discussed above, two similar MTJs were considered. The first MTJ was left as it was and an STO could be engineered on top of the second MTJ to form a stacked STOMTJ DEVICE. The first MTJ and the STOMTJ device were electrically characterized to know the critical current. The scheme discussed above is applicable only if the magnetization of the free layer of the MTJ exhibits precessional motion without the dynamic polarizer.

For the simulated STOMTJ device shown in Figure 1(b), the critical current found was  $i_c = 0.1$  mA. The simulations were repeated for different frequencies of the dynamic polarizer. It was found that the magnetization  $\mathbf{m}$  switches even for 8 GHz as shown in Figure 5. From the results shown in Figure 6, the switching probability  $P_s$  of the free layer magnetization has a maximum at an optimal frequency range of 7 GHz to 8 GHz. The free layer magnetization can be reversed from one state to the other at a frequency close to the mean frequency  $f_s$ . This result offers a frequency-based switching of the free layer magnetization. By adding the dynamic polarizer  $\mathbf{m}_{p2}$  oscillating within an optimal frequency range, it is possible to switch the magnetization of a memory layer in an MRAM device. For better functionality of the device memory, a narrow distribution of switching probability is required. It is important that the switching happens only at one characteristic frequency.

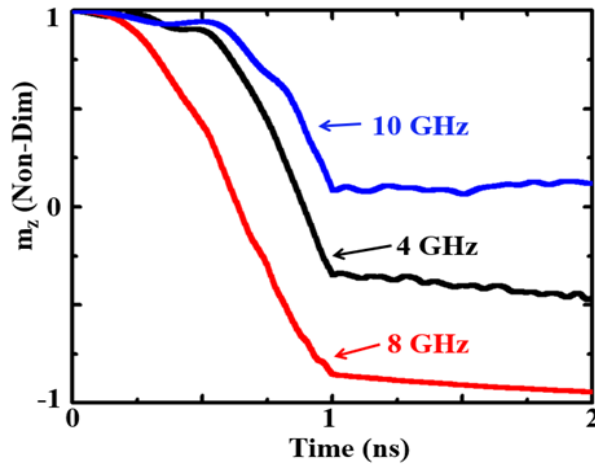


**Figure 5.** Time domain plot of the normalized component of the magnetization  $m_z$  for  $i = 0.1$  mA

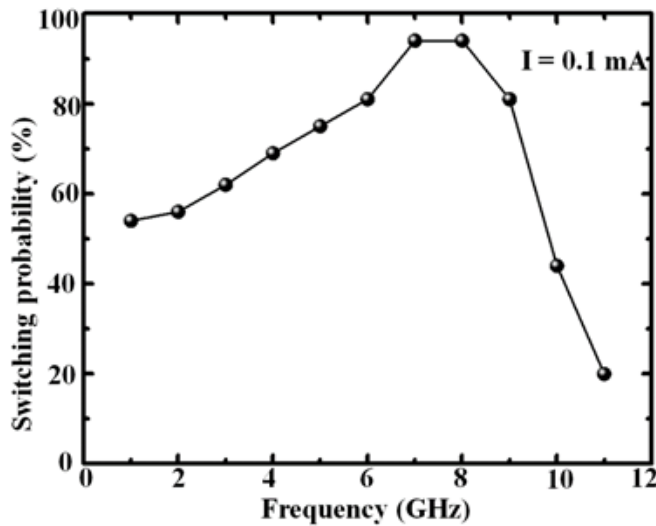


**Figure 6.** Switching probability of the free layer magnetization versus the frequency of the dynamic polarizer for spin-polarized current value  $i = 0.1$  mA. The applied current duration is 2 ns.

#### 4. Conclusion

In summary, we have simulated the STOMTJ device which can be used to attain a low power magnetic memory. The free layer magnetization switching with lower current becomes possible as reported in Figure 3 where the switching probability reaches a maximum when the oscillating polarizer  $\mathbf{m}_{p2}$  is added. A good comparison of the switching process in the MTJ with and without dynamic polarizer is shown. The assist mechanism shown can help reduce high current density without compromising the diameter of the MTJ.

#### Conflict of interest

The authors declare no conflict of interest.

#### Acknowledgement

The authors would like to thank Sultan Qaboos University for the financial support under the grant number IG/SCI/PHYS/18/04.

#### References

- Slonczewski, J.C. Current-driven excitation of magnetic multilayers, *Journal of Magnetism and Magnetic Materials*, 1996, **159**, L1–L7.
- Berger, L. Emission of spin waves by a magnetic multilayer traversed by a current, *Physical Review B*, 1996, **54**, 9353.
- Tsoi, M., Jansen, A.G.M., Bass, J., Chiang, W.C., Seck, M., Tsoi, V., and Wyder, P. Excitation of a magnetic multilayer by an electric current, *Physical Review Letters*, 1998, **80**, 281.
- Myers, E.B., Ralph, D.C., Katine, J.A., Louie, R.N. and Buhrman, R.A. Current-induced switching of domains in magnetic multilayer devices, *Science*, 1999, **285**, 867-870.
- Katine, J.A., F.J. Albert, R.A. Buhrman, Myers, E.B. and Ralph, D.C. Current-Driven Magnetization Reversal and Spin-Wave Excitations in Co/Cu/Co Pillars, *Physical Review Letters*, 2000, **84**, 3149.
- Mangin, S., Ravelosona, D., Katine, J.A., Carey, M.J., Terris, B.D. and Fullerton, E.E. Current-induced magnetization reversal in nanopillars with perpendicular anisotropy, *Nature Materials*, 2006, **5**, 210-215.
- Law, R., Sbiaa, R., Liew, T. and Chong, T.C. Magnetoresistance and switching properties of Co-Fe/Pd-based perpendicular anisotropy single- and dual-spin valves, *IEEE Transactions on Magnetics*, 2008, **44**, 2612.
- Ikeda, S., Miura, K., Yamamoto, H., Mizunuma, K., Gan, H. D., Endo, M., Kanai, S., Hayakawa, J., Matsukura, F. and Ohno, H. A perpendicular-anisotropy CoFeB-MgO magnetic tunnel junction, *Nature Materials*, 2010, **9**, 721-724.
- Yakushiji, K., Saruya, T., Kubota, H., Fukushima, A., Nagahama, T., Yuasa, S. and Ando, K. Ultrathin Co/Pt and Co/Pd superlattice films for MgO-based perpendicular magnetic tunnel junctions, *Applied Physics Letters*, 2010, **97**, 232508.
- Meng, H., Sbiaa, R., Wang, C.C., Lua, S.Y.H. and Akhtar, M.A.K. Annealing temperature window for tunneling magnetoresistance and spin torque switching in CoFeB/MgO/CoFeB perpendicular magnetic tunnel junctions, *Journal of Applied Physics*, 2011, **110**, 103915.
- Khalili Amiri, P., Zeng, Z.M., Langer, J., Zhao, H., Row-Lands, G., Chen, Y.-J., Krivorotov, I.N., Wang, J.P., Jiang, H.W., Katine, J.A., Huai, Y., Galatsis, K. and Wang, K.L. Switching current reduction using perpendicular anisotropy in CoFeB–MgO magnetic tunnel junctions, *Applied Physics Letters*, 2011, **98**, 112507.
- Wang, C.C., Bin Akhtar, M.A.K., Sbiaa, R., Meng, H., Sunny, L.Y.H., Kai, W.S., Ping, L., Carlberg, P. and Arthur, A.K.S. Size dependence effect in MgO-based CoFeB tunnel junctions with perpendicular magnetic anisotropy, *Japanese Journal of Applied Physics*, 2012, **51**, 013101.
- Liu, Y., Yu, T., Zhu, Z., Zhong, H., Khamis, K.M. and Zhu, K. High thermal stability in W/MgO/CoFeB/W/CoFeB/W stacks via ultrathin W insertion with perpendicular magnetic anisotropy, *Journal of Magnetism and Magnetic Materials*, 2016, **410**, 123-127.
- Cuchet, L., Rodmacq, B., Auffret, S., Sousa, R.C., Prejbeanu, I.L. and Dieny, B. Perpendicular magnetic tunnel junctions with a synthetic storage or reference layer: A new route towards Pt- and Pd-free junctions, *Scientific Reports*, 2016, **6**, 21246.
- Honjo, H., Ikeda, S., Sato, H., Watanebe, T., Miura, S., Nasuno, T., Noguchi, Y., Yasuhira, M., Tanigawa, T., Koike, H., Muraguchi, M., Niwa, M., Ito, K., Ohno, H. and Endoh, T. Origin of variation of shift field via annealing at 400°C in a perpendicular-anisotropy magnetic tunnel junction with [Co/Pt]-multilayers based synthetic ferrimagnetic reference layer, *AIP Advances*, 2017, **7**, 055913.
- Sbiaa, R. and Piramanayagam, S.N. Recent developments in dpin transfer torque MRAM, *Physica Status Solidi-RRL*, 2017, **11**, 1700163.
- Krivorotov, I.N., Emley, N.C., Sankey, J.C., Kiselev, S.I., Ralph, D.C. and Buhrman, R.A. Time-domain measurements of nanomagnet dynamics driven by spin-transfer torques, *Science*, 2005, **307**, 228.

18. Rippard, W., Pufall, M., Kaka, S., Russek, S. and Silva, T. Direct-Current Induced Dynamics in  $\text{Co}_{90}\text{Fe}_{10}/\text{Ni}_{80}\text{Fe}_{20}$  Point Contacts, *Physical Review Letters*, 2004, **92**, 027201.
19. Von Kim, J. Spin-Torque Oscillators, in *Solid State Physics*, Elsevier, 2012, **63**, 217-294.
20. Kiselev, S.I., Sankey, J.C., Krivorotov, I.N., Emley, N.C., Rinkoski, M., Perez, C., Buhrman, R.A. and Ralph D.C. Current-induced nanomagnet dynamics for magnetic fields perpendicular to the sample plane, *Physical Review Letters*, 2004, **93**, 036601.
21. Bertotti, G., Serpico, C., Mayergoyz, I.D., Magni, A., D'Aquino, M. and Bonin, R. Magnetization switching and microwave oscillations in nanomagnets driven by spin-polarized currents, *Physical Review Letters*, 2005, **94**, 1.
22. Mistral, Q., Kim, Joo-Von, Devolder, T., Crozat, P. and Chappert, C. Current-driven microwave oscillations in current perpendicular-to-plane spin-valve nanopillars, *Applied Physics Letters*, 2006, **88(19)**, 6-9.
23. Stiles, M. D. and Miltat, J. Spin-transfer torque and dynamics, in *Spin Dynamics in Confined Magnetic Structures III. Topics in Applied Physics*, Springer, 2006, **101**, 225-308.
24. Kläui, M, H. Ehrke, U. Rüdiger, T. Kasama and R. E. Dunin-Borkowski, D. Backes, L. J. Heyderman, C.A.F. Vaz and J.A.C. Bland, G. Faini and E. Cambril, and W. Wernsdorfer, Direct observation of domain-wall pinning at nanoscale constrictions, *Applied Physics Letters*, 2005, **87**, 102509.
25. Hayashi, M., Thomas, L., Rettner, C., Moriya, R., Jiang, X. and Parkin, S.S.P. Dependence of Current and Field Driven Depinning of Domain Walls on Their Structure and Chirality in Permalloy Nanowires, *Physical Review Letters*, 2006, **97**, 207205.
26. Petit, D., Jausovec, A.V., Read, D. and Cowburn, R.P.J. Domain wall pinning and potential landscapes created by constrictions and protrusions in ferromagnetic nanowires, *Journal of Applied Physics*, 2008, **103**, 114307.
27. Parkin, S.S.P., Hayashi, M. and Thomas, L. Magnetic Domain-Wall Racetrack Memory, *Science*, 2008, **320**, 190.
28. Huang, S.H. and Lai, C.H. Domain-wall depinning by controlling its configuration at notch, *Applied Physics Letters*, 2009, **95**, 032505.
29. Bogart, L.K., Atkinson, D., O'Shea, K., Mcgrouter, D. and Mcvitie, S. Dependence of domain wall pinning potential landscapes on domain wall chirality and pinning site geometry in planar nanowires, *Physical Review B*, 2009, **79**, 054414.
30. Sbiaa, R. and Piramanayagam, S.N. Multi-level domain wall memory in constricted magnetic nanowires, *Applied Physics A*, 2014, **114**, 1347.
31. Van De Wiele, B., Laurson, L., Franke, K.J.A. and Van Dijken, S. Electric field driven magnetic domain wall motion in ferromagnetic-ferroelectric heterostructures, *Applied Physics Letters*, 2014, **104**, 012401.
32. Kim, J.S., Mawass, M.A., Bisig, A., Krüger, B., Reeve, R.M., Schulz, T., Büttner, F., Yoon, J., You, C.Y., Weigand, M., Stoll, H., Schütz, G., Swagten, H.J.M., Koopmans, B., Eisebitt, S. and Kläui, M. Synchronous precessional motion of multiple domain walls in a ferromagnetic nanowire by perpendicular field pulses, *Nature Communications*, 2014, **5**, 3429.
33. Al Bahri, M. and Sbiaa, R. Geometrically pinned magnetic domain wall for multi-bit per cell storage memory, *Scientific Reports*, 2016, **6**, 28590.
34. Berganza, E., Bran, C., Jaafar, M., Vázquez, M. and Asenjo, A. Domain wall pinning in FeCoCu bamboo-like nanowires, *Scientific Reports*, 2016, **6**, 29702.
35. Borie, B., Kehlberger, A., Wahrhusen, J., Grimm, H. and Kläui, M. Geometrical Dependence of Domain-Wall Propagation and Nucleation Fields in Magnetic-Domain-Wall Sensors, *Physical Review Applied*, 2017, **8**, 024017.
36. Jin, T., Kumar, D., Gan, W., Ranjbar, M., Luo, F., Sbiaa, R., Liu, X., Lew, W.S. and Piramanayagam, S.N. Nanoscale compositional modification in Co/Pd multilayers for controllable domain wall pinning in race track memory, *Physica Status Solidi-RRL*, 2018, **12**, 1800197.
37. Choi, H.S., Kang, S.Y., Cho, S.J., Oh, I.Y., Shin, M., Park, H., Jang, C., Min, B.C., Kim, S.I., Park, S.Y. and Park, C.S. Spin nano-oscillator-based wireless communication, *Scientific Reports*, 2014, **4**, 5486.
38. Sbiaa, R. Magnetization reversal dependence on magnetic properties of a spin torque oscillator with in-plane anisotropy free layer and orthogonal polarizer, *Current Applied Physics*, 2014, **14**, 1521.
39. Sbiaa, R. Magnetization reversal driven by a spin torque oscillator, *Applied Physics Letters*, 2014, **105**, 092407.
40. Sbiaa, R. Frequency selection for magnetization switching in spin torque magnetic memory, *Journal of Physics: D, Applied Physics*, 2015, **48**, 195001.
41. Rahman, N. and Sbiaa, R. Thickness dependence of magnetization dynamics of an in-plane anisotropy ferromagnet under a crossed spin torque polarizer, *Journal of Magnetism and Magnetic Materials*, 2017, **439**, 95.

---

Received 4 August 2019

Accepted 3 October 2019